EPITAXIAL FERROMAGNETIC MnGa AND (MnNi)Ga THIN FILMS WITH PERPENDICULAR MAGNETIZATION ON GaAs

M. TANAKA[a)], J.P. HARBISON, T.D. SANDS, B.A. PHILIPS[b)], J. DE BOECK[c)], T.L. CHEEKS, L.T. FLOREZ and V.G. KERAMIDAS
Bellcore, 331 Newman Springs Road, Red Bank, NJ 07701-7040.
[a)]*On leave from Department of Electrical Engineering, The University of Tokyo, 7-3-1 Hongo, Bunkyo-ku, Tokyo 113, Japan.*
[b)]*Present address: Materials Science Department, Carnegie Mellon University, Pittsburgh, PA 15213-3890.*
[c)]*Permanent address: Interuniversity Microelectronics Center (IMEC), Kapeldreef 75, B3001 Leuven, Belgium.*

ABSTRACT

We have successfully grown thermodynamically stable ferromagnetic Mn_xGa_{1-x} (x=0.55~0.60) thin films with thicknesses ranging from 3 nm to 60 nm on GaAs substrates by molecular beam epitaxy. The c-axis of the tetragonal structure of the MnGa film is shown to be aligned perpendicular to the substrate. Both magnetization measurements and extraordinary Hall effect measurements indicate perpendicular magnetization of the MnGa films, exhibiting square-like hysteresis characteristics. Furthermore, we have investigated the effect of Ni additions as a substitution for Mn in $(Mn_{60-y}Ni_y)Ga_{40}$ alloy thin films with y=0 - 30 at% Ni. With increasing Ni, the perpendicular component of the magnetization becomes smaller up to y=18 where the magnetization is in-plane. At y=30, the magnetization is again perpendicular.

INTRODUCTION

Epitaxial growth of ferromagnetic thin films on III-V semiconductors can lead to the integration of magnetic effects with high speed III-V electronics/photonics [1], offering a wide range of possibilities for producing new devices such as non-volatile memory coupled with underlying III-V circuitry. Although most of the magnetic thin films so far obtained have in-plane magnetization due to the shape anisotropy [2], many potential applications of ferromagnetic films require magnetization perpendicular to the substrate, both to allow higher storage density in magnetic storage applications and to allow the use of extraordinary Hall effect (EHE) and magneto-optic Kerr effect (MOKE).

Recently, we have explored the growth of metastable τMnAl on GaAs substrates by molecular beam epitaxy (MBE), and found that heteroepitaxy helps to align the magnetization direction of the MnAl film, which lies along the c-axis of the tetragonal unit cell of τ phase, in an orientation perpendicular to the substrate [3][4]. In this paper, we present our study of the MBE growth of Mn_xGa_{1-x} (x=0.55 - 0.60), the stable ferromagnetic Ga-based phase, compatible with GaAs substrates in epitaxy due to the shared group III atom in the MnGa/GaAs couple. It is shown that the MBE-grown MnGa films indeed have perpendicular magnetization, square-like EHE hysteresis characteristics, and a high value of remanent magnetization, making them a promising candidate for applications in certain non-volatile magnetic memory coupled with III-V optical and/or electronic devices. Furthermore, we have investigated the MBE growth of $(Mn_{60-y}Ni_y)Ga_{40}$ alloy films with y=0 - 30 at % Ni and the dependence of the magnetic properties on the Ni composition.

MBE GROWTH

Unlike metastable τMnAl, Mn_xGa_{1-x} with x=0.55 - 0.60 is a thermodynamically stable ferromagnetic phase in the bulk Mn-Ga system [5][6]. In the bulk, the single phase region was found to extend from 54.5 to 60.0 at% Mn at 450°C [6]. The crystal structure of the MnGa is tetragonal, analogous to that of τMnAl, with an ordered crystal structure of the CuAu type. The Mn-Mn spacing in the basal plane (a_0) is 0.274nm, independent of the Mn content, and along the c-axis (c_0) is 0.365nm at 56% Mn and 0.369 nm at 59% Mn, respectively. The easy magnetization direction is along the c-axis. Since a_0 is close to half of the lattice constant of GaAs (0.283nm) with a lattice mismatch of only 3.8%, the orientation relationship with the c-axis of the MnGa parallel to the surface normal of the (001) GaAs substrates is expected, as

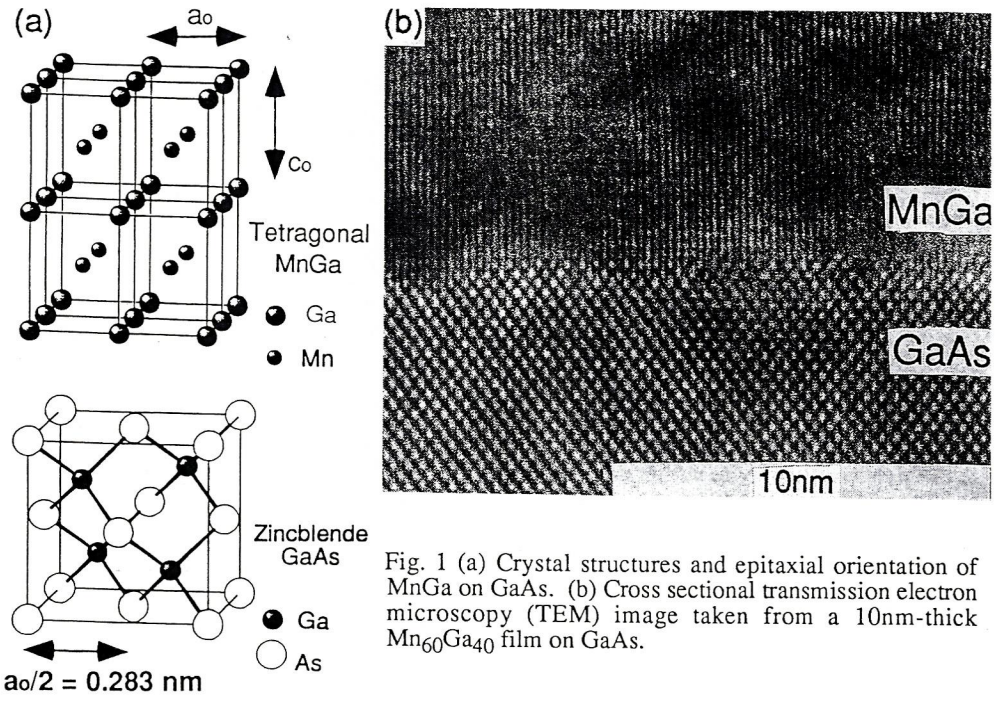

Fig. 1 (a) Crystal structures and epitaxial orientation of MnGa on GaAs. (b) Cross sectional transmission electron microscopy (TEM) image taken from a 10nm-thick $Mn_{60}Ga_{40}$ film on GaAs.

shown in Fig. 1 (a).

The growth of MnGa on (001) GaAs was performed with a conventional III-V MBE machine (Riber-2300) with effusion cells for Mn, Ni, Ga and As, using the multistep technique analogous to that employed in the growth of τMnAl/AlAs/GaAs [3][4]. Since the details of the growth have been reported previously [7], we briefly summarize the growth procedure here. After a 100nm-thick GaAs buffer layer was grown at 580°C under conventional III-V growth conditions, the substrate temperature was cooled to 20 - 40°C while completely eliminating the As flux. Then a thin (about 0.9nm-thick) amorphous MnGa template was deposited at 20 - 40°C. The amorphous template was next heated up to 200 - 250°C to form a monocrystalline template by solid phase epitaxy. After the template with the desired epitaxial relation was thus established, Mn and Ga were subsequently codeposited at 150 - 200°C at a growth rate of 0.05μm/hr, to a final Mn_xGa_{1-x} thickness of 3 - 60nm. The Mn content x was set to 55% - 60% in the present study. Finally, postgrowth annealing was performed at 300 - 410°C for 2 minutes. Such annealing at a temperature T_a of at least 300°C was found to be necessary in order to improve the structural and magnetic properties of the MnGa film.

STRUCTURAL AND MAGNETIC PROPERTIES OF MnGa THIN FILMS

The epitaxial MnGa with its *c*-axis aligned normal to the substrate was confirmed first by *in situ* reflection high energy electron diffraction (RHEED) and also by cross sectional transmission electron microscopy (TEM). Figure 1 (b) shows a <110> TEM lattice image of the 10nm-thick $Mn_{60}Ga_{40}$ film grown on GaAs, indicating that a monocrystalline MnGa layer was indeed grown with the *c*-axis properly oriented perpendicular to the GaAs substrate. The interface between the MnGa and the GaAs is found to be very smooth and abrupt, and no interfacial transition layer was observed. The horizontal lattice fringes with a spacing of 0.31nm correspond to the (001) planes of the tetragonal structure of the MnGa. This value of the *c* parameter in the present epitaxial MnGa film is significantly smaller than that of bulk MnGa (0.36~0.37nm) [5][6] and a MBE-grown MnGa film (0.35nm) with greater (30nm) thickness [8]. Although the reason for the reduced tetragonality is not yet clear, the explanation may be that the present MBE film is

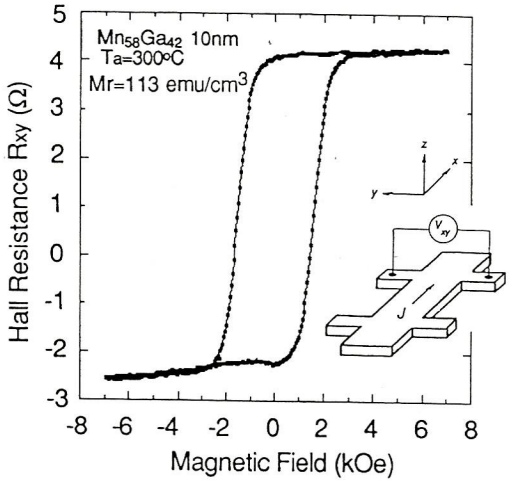

Fig. 2 Extraordinary Hall effect (EHE) as a function of perpendicular magnetic field for a 10nm-thick $Mn_{58}Ga_{42}$ film at room temperature. The inset shows the geometry of the measurement. The M_r value perpendicular to the film plane is also shown.

composed of an intermediate phase between the tetragonal phase and cubic phase, stabilized by the coherent epitaxy, as has been shown in the case of MnNiAl [9][10].

To investigate the magnetic properties of the epitaxial MnGa films, we performed vibrating sample magnetometer (VSM) measurements as a function of magnetic field perpendicular to the substrate at room temperature. Fairly square hysteresis loops were observed at room temperature [7], offering direct evidence of the desired perpendicular magnetization. Similar results were obtained in all the samples of MnGa with Mn content ranging from 55% to 60%. The remanent magnetization M_r along the c-axis was estimated to be 113 - 225 emu/cm^3, and the coercive field H_c was 0.85 - 3.15 kOe.

The Hall effect measured in a ferromagnetic film is known to have an "extraordinary" component resulting from the asymmetric scattering of carriers with magnetic atoms [11]. The extraordinary Hall effect (EHE) is very useful in this case because the Hall resistivity measured in a patterned Hall bar in the MnGa films is proportional to the magnetic moment perpendicular to the film plane. Figure 2 shows an example of Hall resistance R_{xy} vs. perpendicular magnetic field measured at room temperature on a 200μm-wide Hall bar fabricated in a 10nm-thick $Mn_{58}Ga_{42}$ film prepared with T_a = 300°C. One can see a fairly square hysteresis loop with nearly 100% remanence, Hall resistance R_{xy} of 3.5 Ω (corresponding Hall resistivity ρ_{xy} of 3.5 μΩcm) and H_c of 1.46 kOe. Similar square-like hysteresis loops were observed in the EHE measurements in all the present MnGa samples, indicating a large component of perpendicular magnetization, consistent with the VSM measurement results. The EHE resistivity ρ_{xy} was found to vary from 0.1 μΩcm to 4 μΩcm, depending on the growth parameters.

The magnetic and magnetotransport properties of the MBE-grown MnGa films, such as remanent magnetization M_r, saturation magnetization M_s, coercive field H_c , Hall resistance R_{xy} and Hall resistivity ρ_{xy}, depend on the various growth parameters such as growth temperature T_g, postgrowth annealing temperature T_a, Mn composition x, and thickness of the MnGa film t. Here, we briefly describe the change in the properties of $Mn_{60}Ga_{40}$ films grown at T_g=200°C and at T_a = 350°C when the thickness t was varied from 3 nm to 60 nm. Over the entire range of the thickness explored here, perpendicular magnetization was evidenced by both VSM and EHE measurements and electrical continuity in each of the films was confirmed. Figure 3 shows a set of plots of Hall resistance as a function of perpendicular magnetic field at room temperature on the $Mn_{60}Ga_{40}$ films with t=3nm (a), 10nm (b), and 60nm (c). With the change of film thickness, the value of R_{xy} ($=\rho_{xy}/t$) changes drastically, from about 2 Ω to 0.07 Ω. The value of coercive field H_c was maximum (3.15 kOe) at t=10nm, and minimum (0.85 kOe) at t=60nm. The VSM measurement showed that the saturation magnetization M_s of the 60nm-thick film was 394 emu/cm^3, as high as the bulk value of 390emu/cm^3 [6], indicating the high quality of the MBE film. This growth parameter dependence can allow us to control the magnetic properties in these MBE-grown films.

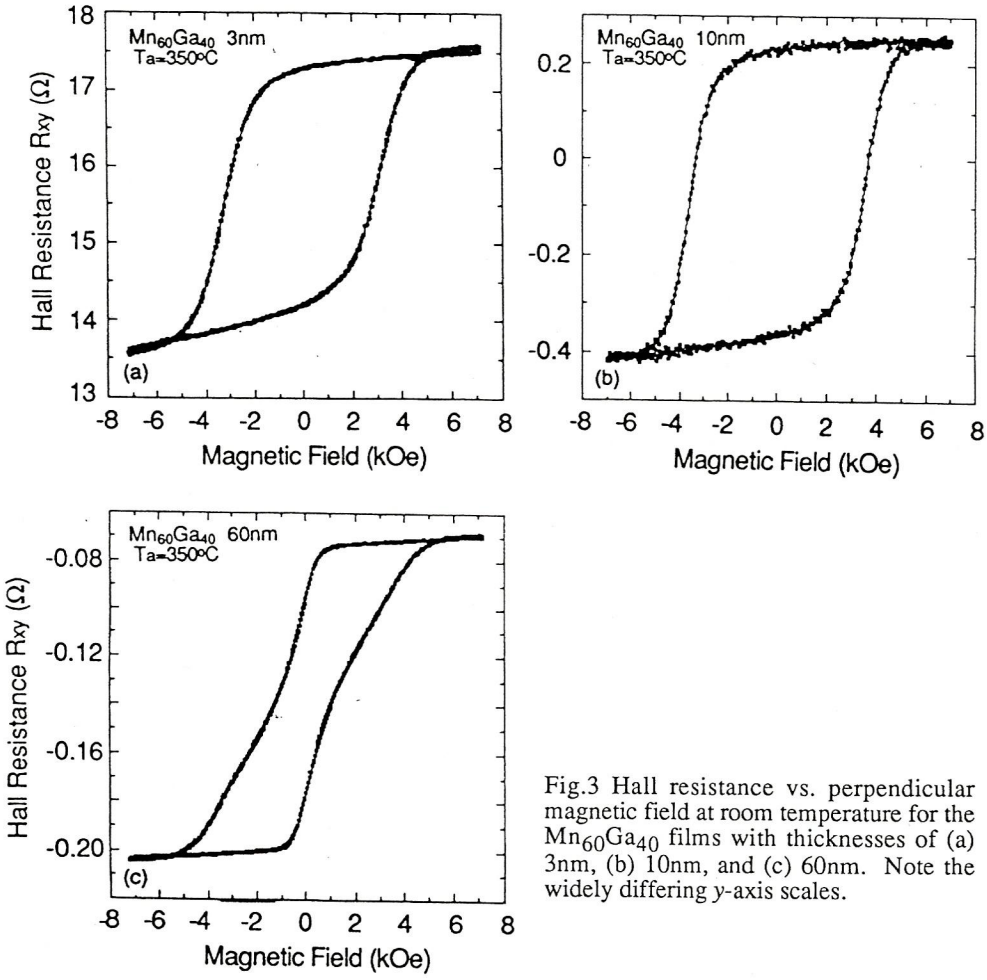

Fig.3 Hall resistance vs. perpendicular magnetic field at room temperature for the $Mn_{60}Ga_{40}$ films with thicknesses of (a) 3nm, (b) 10nm, and (c) 60nm. Note the widely differing *y*-axis scales.

Ni ADDITIONS: $(Mn_{60-y}Ni_y)Ga_{40}$ ALLOY THIN FILMS

The addition of Ni to the MnGa films is expected to lead to the reduction of the tetragonality of the lattice. This should in turn decrease the magnetocrystalline anisotropy, resulting in a change in magnetic properties, as in the case of MnNiAl thin films [9]. In order to explore the effect of Ni additions on the structural and magnetic properties, we have fabricated a series of (MnNi)Ga samples where Ni was substituted for Mn in $Mn_{60}Ga_{40}$ films over the range of 4% to 30% atomic fraction of Ni. The growth procedures and conditions in the MnNiGa films are the same as in the case of MnGa, except that the growth temperature was 200 - 220°C, a little higher than that of MnGa.

Figure 4 shows a series of RHEED patterns along the <110> azimuth taken from the 10nm-thick $(Mn_{60-y}Ni_y)Ga_{40}$ films with various Ni content (y=4, 8, 18 and 30 at% Ni), both for as-grown surfaces and for the surfaces after the postgrowth annealing at 300°C for 2 minutes. These streaky patterns suggest that monocrystalline epitaxial films are obtained with very smooth surfaces over the entire range explored here. The postgrowth annealing was found to be effective in improving the RHEED quality. As the value of y increases, the RHEED pattern becomes more streaky and sharper. For the MnNiGa with y=30, one can see a (4x4) reconstruction on the as grown surface which changed into a sharp (2x2) reconstruction after the annealing, while (2x2) reconstructions are seen for the MnNiGa with y<30.

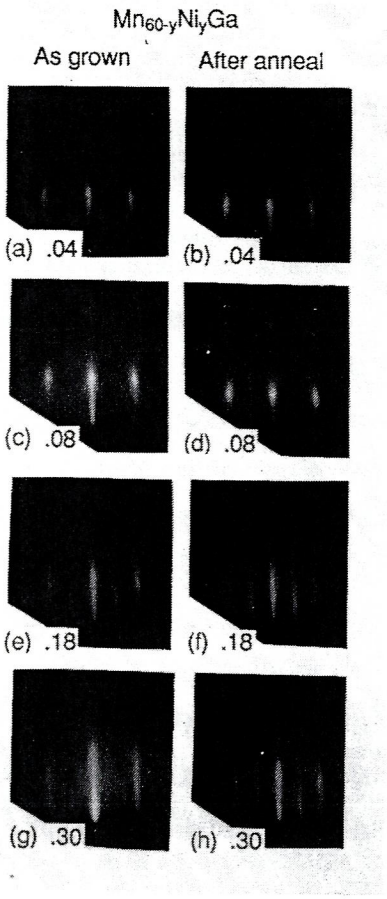

Fig. 4 A series of RHEED patterns along the <110> azimuth taken of 10nm-thick $(Mn_{60-y}Ni_y)Ga_{40}$ films with various Ni content (y=4, 8, 18 and 30 at % Ni as indicated). The left hand pictures are taken from the as grown surfaces, and right hand ones are from the surfaces after the postgrowth annealing at 300°C for 2 minutes.

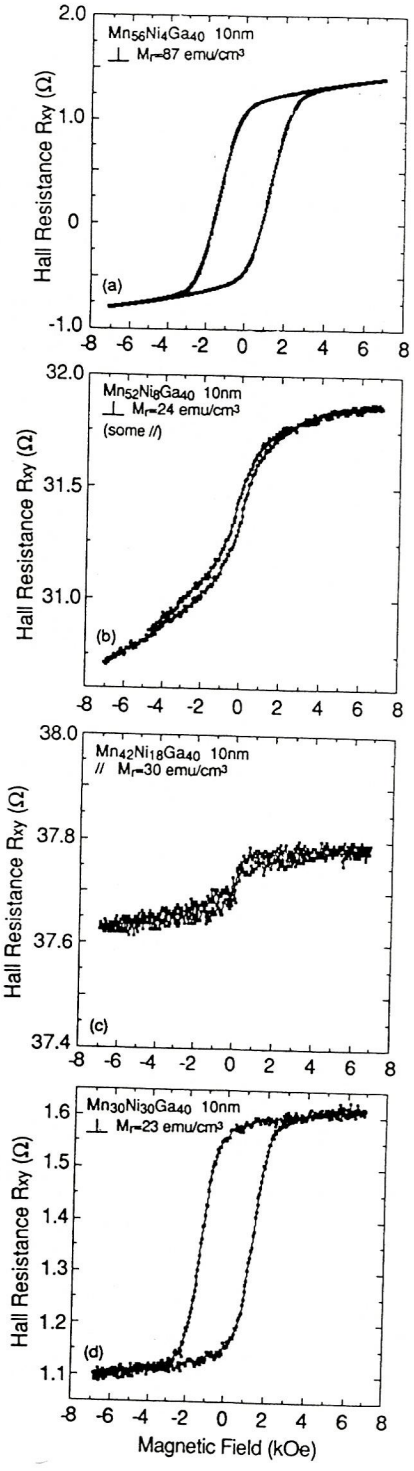

Fig. 5 EHE characteristics are plotted as a function of applied magnetic field perpendicular to the film plane, and the M_r values are shown with the magnetization directions, where ⊥ and // denote perpendicular and in-plane magnetization, respectively.

To investigate the magnetic properties, we performed VSM and EHE measurements at room temperature. The results are summarized in Fig. 5, where the EHE characteristics are plotted as a function of magnetic field applied perpendicular to the film plane. The M_r values and the magnetization directions measured by VSM are also shown in the figures. It was found that the perpendicular magnetization decreases and the EHE hysteresis loop becomes smaller with increasing Ni content (y varing from 0 to 18), as shown in Fig. 2 and Figs. 5 (a), (b) and (c). The VSM measurements revealed that the MnNiGa films with y=4 and y=8 have smaller values of M_r (87 emu/cm^3 and 24 emu/cm^3, respectively), along the perpendicular direction, than the M_r (> 110 emu/cm^3) of MnGa. However, it was found that the MnNiGa film with y=8 has some in-plane component of magnetization though the dominant component is perpendicular. It was also found that the MnNiGa film with y=18 has almost no perpendicular magnetization, but rather a dominantly in-plane magnetization. This result suggests that the epitaxial relationship of Fig.1 (a) may not be realized in the $Mn_{42}Ni_{18}Ga_{40}$/GaAs heterostructure, and the c-axis of the MnNiGa may instead be aligned in the (001) plane of GaAs. Alternatively, the magneto-crystalline anisotropy may be overcome by the shape anisotropy, yielding in-plane magnetization. This could result from the reduced tetragonality of the MnNiGa with such a high Ni content, though a more detailed structural analysis is necessary. Furthermore, it was found that when we further increase the Ni addition up to y=30, the MnNiGa shows perpendicular magnetization and a square-like EHE hysteresis loop again, as shown in Fig. 5 (d), though both the values of M_r and ρ_{xy} are significantly smaller than those of MnGa. Thus the Ni content dependence of the magnetic properties of the MnNiGa alloy films was found to be more complex than that of MnNiAl alloy films [9].

CONCLUSIONS

We have successfully grown ferromagnetic MnGa films on GaAs by MBE. The long axis (c-axis) of the tetragonal structure of the MnGa film is aligned perpendicular to the substrate. Both VSM and EHE measurements confirm this perpendicular magnetization, and exhibit square-like hysteresis loops in our MnGa films with thicknesses ranging from 3nm to 60nm at room temperature. The growth and magnetic properties of $Mn_{60-y}Ni_yGa_{40}$ alloy films on GaAs were also explored. With increasing Ni, the perpendicular component of the magnetization becomes smaller and the alloy film at y=18 shows in-plane magnetization, while the film at y=30 shows perpendicular magnetization.

ACKNOWLEDGMENTS

The authors thank the cooperation of M.C. Tamargo and H.L. Gilchrist. One of the authors (M.T.) acknowledges the financial support from the Japan Society for the Promotion of Science.

REFERENCES

1. G.A. Prinz, Science **250**, 1092 (1990).
2. J.J. Krebs, Appl. Phys. **A49**, 513 (1989).
3. T. Sands, J.P. Harbison, M.L. Leadbeater, S.J. Allen, Jr., G.W. Hull, R. Ramesh, and V.G. Keramidas, Appl. Phys. Lett. **57**, 2609 (1990).
4. J.P. Harbison, T. Sands, R. Ramesh, L.T. Florez, B.J. Wilkens, and V.G. Keramidas, J. Crystal Growth **111**, 978 (1991).
5. T.A. Bither and W.H. Cloud, J. Appl. Phys. **36**, 1501 (1965).
6. M. Hasegawa and I. Tsuboya, Review of Electrical Communication Laboratory **16**, 605 (1968) and references therein.
7. M. Tanaka, J.P. Harbison, J. DeBoeck, T. Sands, B. Philips, T.L. Cheeks , V.G. Keramidas, Appl. Phys. Lett. **62**, 1565 (1993).
8. K.M. Krishnan, Appl. Phys. Lett. **61**, 2365 (1992).
9. J.P. Harbison, T. Sands, J. DeBoeck, T.L. Cheeks, P. Miceli, M. Tanaka, L.T. Florez, B.J. Wilkens, H.L. Gilchrist and V.G. Keramidas, J. Crystal Growth, in press.
10. T. Sands, J. DeBoeck, J.P. Harbison, A. Scherer, H.L. Gilchrist, T.L. Cheeks, P.F. Miceli, R. Ramesh and V.G. Keramidas, J. Appl. Phys., in press.
11. E.D. Dahlberg, K. Riggs and G.A. Prinz, J. Appl. Phys. **63**, 4270 (1988).